Global Journal of Engineering and Technology Advances
eISSN: 2582-5003
Cross Ref DOI: 10.30574/gjeta
Journal homepage: https://gjeta.com/

(RESEARCH ARTICLE)

Check for updates

Feasibility study of an interconnection of electrical energy transmission networks: Case study of 4 countries in Central Africa and Nigeria

Romain Platinie KUEDA *, André YOUMSSI and Ndjiya Ngasop

Department of Electrical Engineering, Energy and Automation, National School of Agro-Industrial Sciences (ENSAI), University of Ngaoundere, Cameroon.

Global Journal of Engineering and Technology Advances, 2025, 23(03), 180-199

Publication history: Received on 21 April 2025; revised on 04 June 2025; accepted on 06 June 2025

Article DOI: https://doi.org/10.30574/gjeta.2025.23.3.0182

Abstract

With the current trend and progress in science, the production of electrical energy can be done in one country and consumed in another. Central Africa is experiencing a paradoxical situation characterized, among other things, by low hydroelectric production, an electrification rate of 13% compared to 90% in North Africa and a very low level of interconnection of its electricity networks. Thus, the interconnection of the networks of the countries of Central Africa and Nigeria will aim not only to facilitate the energy integration of the sub-region but also to reduce the inconvenience caused to the populations of the sub-region. This study focuses on the feasibility of an interconnection between 4 countries in Central Africa (Cameroon, Central African Republic, Chad, DRC) and Nigeria by proposing a multi-terminal high voltage direct current transmission system that we simulated under MATLAB/Simulink software.

Keywords: Electric energy; Electric network; Interconnection; High voltage direct current; Power synchronization; Frequency control; Stability and efficiency of HVDC transmission system

1. Introduction

The last century has demonstrated that every facet of human development revolves around a healthy and stable energy supply regime. Electricity has become the primary resource needed in human society, for virtually all aspects of societal development, from industry and commercial applications to domestic use. The electric power system serves to generate, transmit and distribute electrical energy to consumers in an efficient, economical and reliable manner. It is made up of production plants, transmission lines and distribution networks [1] . Along the same lines, an electrical interconnection allows electricity to flow between separate networks, or synchronous networks. They can consist of underwater power cables, underground power cables or overhead power lines [11] . The interconnection of electrical networks not only makes it possible to exchange energy between the different power plants in service but also to switch networks in the event of a source failure. It has many advantages such as [12-14] :

- Optimization of the exploitation of production park resources and use of available power plants at all times to balance demand and production;
- Optimization of savings on operating costs;
- The mitigation of frequency and voltage variations resulting from fluctuations in consumption;
- Improving the production-consumption adequacy by increasing the interconnection capacity between systems and achieving the energy transition;
- Reduction of energy costs;
- Optimization of the security, stability and reliability of interconnected networks;
- Increase in electricity supply.

* Corresponding author: Romain Platinie KUEDA

In the study of the feasibility of interconnections of alternating electrical energy transmission networks, the basic constraints on the synchronization of frequency and voltage must be observed such that the electrical energy transmission networks must have the same frequency, the same voltage and the same transport angle. The Central Africa sub-region is characterized by a very low level of interconnection, representing a real obstacle to its development. For decades, high-voltage alternating current (HVAC) has been the most conventional method of delivering power. With recent advances in power electronics, high-voltage direct current (HVDC) is an established technology in long-distance power transmission. As a result, it is re-emerging as the best option due to improved system operation and better support for the integration of renewable energy. Due to its flexibility, HVDC technology is able to provide the transmission system with several benefits such as improved transfer capacity, better power flow control, improved transient stability, stability/ improved control and absence of production or absorption of reactive power by the line [2] .

Because HVDC electrical power transmission is very attractive, it presents a real problem in terms of its control strategy. This is how many authors have worked on control strategies for HVDC systems with the aim of contributing to improving their performance and stability. In his work, [3] propose the master-slave control strategy for the control of a HVDC system with low reliability because the failure of the "master" converter leads to the total shutdown of the system. To therefore overcome the limits of the master-slave control strategy, [4] and [5] present the voltage drop control strategy where two or more converters are responsible for regulating the voltage in the DC bus and the other converters in the system regulate the power flow. [6] proposed a combined control strategy between the Master Slave Control Strategy (MSCS) and the Voltage Margin Control Strategy (VMCS) with DC voltage oscillations observed due to the MSCS. [7] proposed the power angle control strategy for controlling HVDC systems where it uses the angle and magnitude of the AC voltage at the point of common coupling (PCC) to control the active and reactive power independently. Although the power angle control strategy is interesting and is currently applied in conventional HVAC systems, its major drawback is its inability to limit the currents flowing through the voltage source converter. As a means of circumventing the limit posed by the power angle control strategy, [8] and [2] present the vector control strategy (VCS) having the ability to limit the current flowing through the converter. But the proposed VCS has an inability to connect to weak AC networks because of its phase-locked loop. To therefore deal with the limitations of VCS, [9] and [10] present the power synchronization control strategy (PSCS) where the phase lock loop is replaced by the power synchronization loop. On the other hand, for overall control and for system stability, PSCS does not take into account the frequency control of AC networks.

It is in this context that we propose an improvement of the PSCS by adding to the existing control scheme a frequency control strategy for better stability and efficiency of the HVDC transmission system. The main objective of this study is to carry out an interconnection and solve the problem of stability of electric power transmission networks (SEPT) such as the SEPT of the countries of Central Africa and Nigeria by the new energy transport technology electrical in HVDC.

Our work will therefore be developed in three parts:

- First, we will discuss Modeling of the elements constituting the multi-terminal HVDC system. In this part a complete detail will be given on the power synchronization loop (PSL), the control strategy of the MTDC system and AC voltage control loop.
- Secondly, we will present the material and the main analysis tools on the electrical energy transmission networks of the Central African countries mentioned, and Nigeria.
- Thirdly, we will present the results and therefore the description of the MTDC system of 5 CA countries and Nigeria as well as the interpretations that we will bring to them.
- Finally, all we will have to do is conclude and propose perspectives for future studies to improve this study.

2. Material and methods

In this part, we will present the material and the main analysis tools on the electrical energy transmission networks of the Central African countries mentioned and Nigeria. Table 1 shows the description of the electrical energy transmission networks taking into account the production system, voltage level, frequency and the company in charge of the electrical energy transmission on which the implementation of the model is made.

Table 1 Description of electrical energy transmission networks

N 0	Network	Production		Voltage (kV)	Frequency (Hz)	Company
1	SIN Cameroon	Hydroelectricity (74%)	Fossil energy (26%)	225 / 90	50	SONATREL
2	NIN Cameroon	Hydroelectricity	Fossil fuels	110 / 90	50	SONATREL
3	Nigerian	Hydroelectricity (18.4%)	Fossil energy (81.6%)	330 / 132	50	TCN
4	Chadian	Hydroelectricity (0%)	Fossil energy (100%)	110 / 15	50	SNE
5	Central African	Hydroelectricity (100%)	Fossil energy (0%)	225 / 110 / 90	50	ENERCA
6	DRC	Hydroelectricity (96%)	Fossil energy (4%)	220 / 90	50	SNEL

2.1. Hardware

To carry out this study, we will use:

- An ordinary Hewlett-Packard HP 110-3800 laptop, Inetl ® Atom™ CPU N455 @1.66GHz 1.67 GHz; 1GB RAM.
- MATLAB R2010a data simulation and numerical calculation software.

2.2. Methodology for modeling the elements constituting the multi-terminal HVDC system

2.2.1. Modeling the two-level VSC converter

The mathematical model presented here is that proposed by [23] . Figure **1** shows the circuit diagram of the classic VSC, where u_{sl} and i_{sl} (l = a, b, c) are the AC bus voltages and currents, respectively.

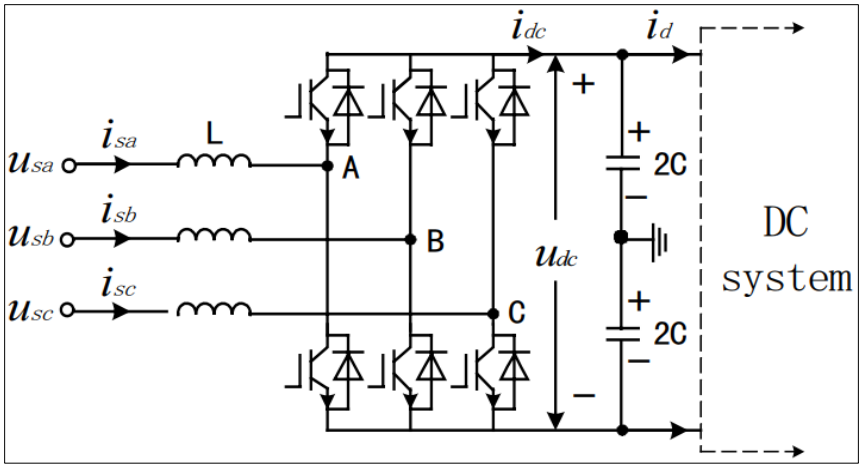

Figure 1 Classic VSC topology with 6 valves

Let us designate by u_{s_abc}, the voltage on the network side and by i_{s_abc}, the current leaving the infinite bus. By applying the mesh laws, we obtain the following system of equations:

$$\begin{cases} L\frac{di_{sa}}{dt} = u_{sa} - u_{ca} - Ri_{ca} \\ L\frac{di_{sb}}{dt} = u_{sb} - u_{cb} - Ri_{cb} \\ L\frac{di_{sc}}{dt} = u_{sc} - u_{cc} - Ri_{cc} \end{cases} \quad \text{(Eq. 1)}$$

Where u_{s_abc} : Represents the network voltage; u_{c_abc} : Line voltage

After simplification by the Park transformation and according to the instantaneous power theory (the active power at the alternating current side is equal to the power at the DC bus), neglecting the converter reactance resistance and the

losses of switching, the active and reactive power on the AC side of the VSC and the active power on the DC side can be respectively expressed by:

$$\begin{cases} P = u_{sd}i_{sd} + u_{sq}i_{sq} \\ Q = u_{sq}i_{sd} - u_{sd}i_{sq} \\ P_{dc} = u_{dc} \cdot i_{dc} \end{cases} \quad \text{……(Eq. 2)}$$

Based on the law of conservation of energy, the active power transferred in the multi-terminal HVDC system must satisfy the following relationship:

$$\sum P = 0 \ldots\ldots\ldots\ldots\ldots \quad \text{(Eq. 3)}$$

2.2.2. DC line modeling

Depending on the purpose of the study, DC cables can be modeled with the distributed model or with the π-circuit model. The distributed model is suitable for transient analysis, while the π-circuit model is used for slower dynamics. The π-circuit model is chosen and the fast dynamics due to DC cable inductances and converter switching are not considered in this study. Figure **2 shows the DC side** of a two-terminal VSC-HVDC system with two cables of opposite voltage level [24] .

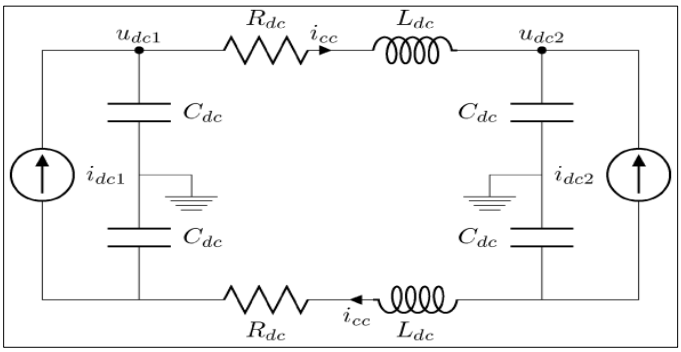

Figure 2 DC circuit of two-terminal VSC-HVDC system

The very simple equations governing this circuit are given by the equation by applying the laws of nodes and meshes:

$$C_{dc}\frac{du_{dc_1}}{dt} = i_{dc_1} - i_{cc} \ldots\ldots\ldots \quad \text{(Eq. 4)}$$

$$C_{dc}\frac{du_{dc_2}}{dt} = i_{dc_2} + i_{cc} \ldots\ldots\ldots\ldots \quad \text{(Eq. 5)}$$

$$L_{dc}\frac{di_{cc}}{dt} = u_{dc_1} - u_{dc_2} - R_{dc}i_{cc} \ldots\ldots\ldots\ldots \quad \text{(Eq. 6)}$$

One converter in an MTDC system can be connected to a number of other converters (**Figure 3**). We set the current directions in the DC lines such that the current from converter *i* to converter *j* is positive if *i* is smaller than *j*. Converter 1 therefore only has incoming currents, and converter *n* only has outgoing currents. For any other converter *i*, there are *n-1* incoming, and *nt* outgoing currents.

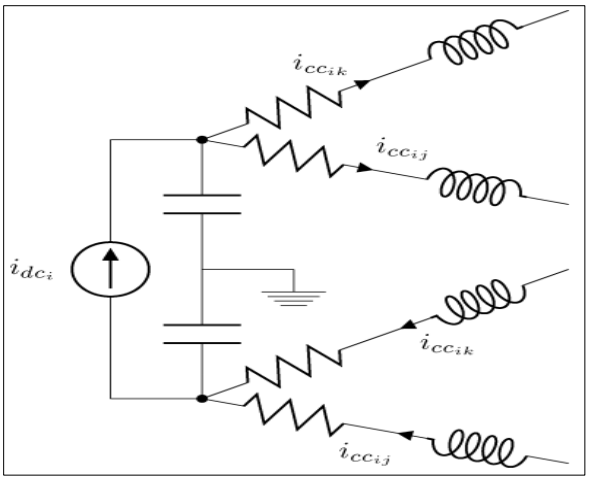

Figure 3 Node in an MTDC circuit

The generalized dynamic equations of any direct current circuit can then be written as follows:

$$C_{dc_i}\frac{du_{dc_i}}{dt} = i_{dc_i} - \sum_{j=i+1}^{n} i_{cc_{ij}} \; Avec\; i = 1..... \quad \text{(Eq. 7)}$$

$$C_{\mathrm{dc}_i}\frac{du_{\mathrm{dc}_i}}{dt} = i_{\mathrm{dc}_i} + \sum_{j=1}^{i-1} i_{\mathrm{cc}_{ji}} - \sum_{j=i+1}^{n} i_{cc_{ij}} \; Avec\; i = 2, \ldots, n-1..... \quad \text{(Eq. 8)}$$

$$C_{dc_i}\frac{du_{dc_i}}{dt} = i_{dc_i} + \sum_{j=1}^{i-1} i_{cc_{ji}} \; avec\; i = n..... \quad \text{(Eq. 9)}$$

$$L_{dc}\frac{di_{cc_{ij}}}{dt} = u_{dc_i} - u_{dc_j} - R_{dc_{ij}} i_{Cc_{ij}} \; \forall j < n, \forall i < j..... \quad \text{(Eq. 10)}$$

MTDC System Control Strategy

The control strategy proposed in this section is a combination of the power synchronization strategy and the frequency control strategy, i.e. a dual control strategy. The overall control structure of the MTDC system is shown in Figure 4:

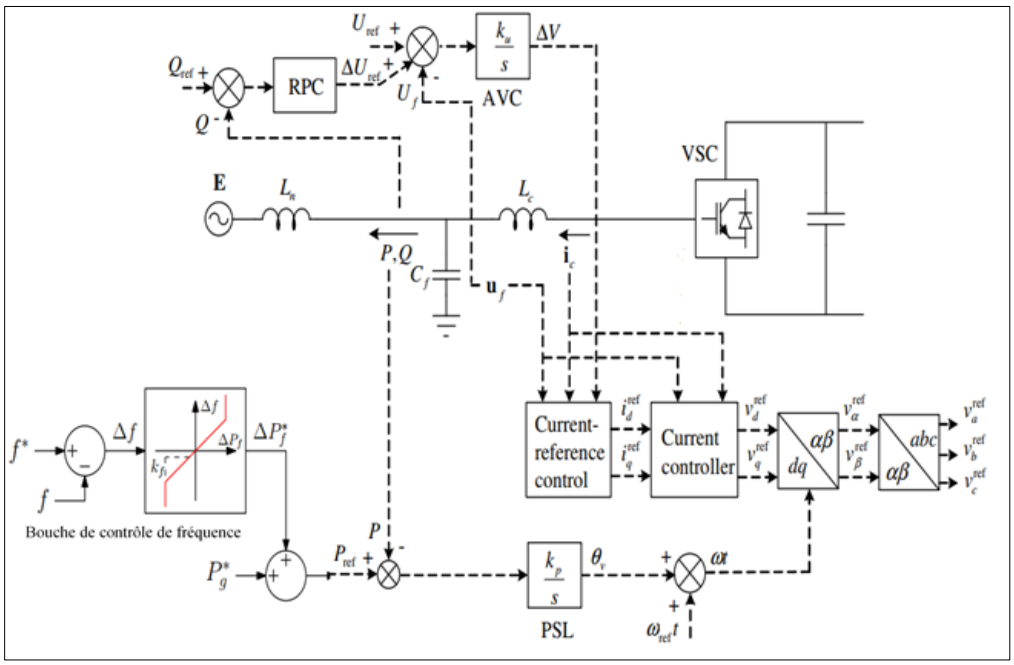

Figure 4 Dual control technique (SCF and SCSP)

2.2.3. Power synchronization loop (PSL)

The power-timing ball is based on equation 11

$$P = \frac{U_1 U_2 sin\theta}{X}$$
$$Q = \frac{U_1^2 - U_1 U_2 cos\theta}{X} \quad \text{(Eq. 11)}$$

With: P and Q the active and reactive powers between two nodes

θ and X are the phase angle difference and line reactance between the two nodes

It maintains synchronism between the VSC and the AC system. This is the active power control loop. The control law is given by equation 12:

$$\frac{d\Delta\theta}{dt} = K_p(P_{ref} - P) \quad \text{(Eq. 12)}$$

Where: P_{ref} is the reference for the active power; P is the active power measured at the VSC output; K_p is the gain of the controller; Δθ is the controller output which directly provides timing for the VSC so no need for a PLL.

2.2.4. Continuous voltage control loop

The PSCS must keep the DC voltage constant to keep the active power flow balanced between the two sides. The control law is given by:

$$P_{ref} = \left(K_{pd} + \frac{K_{id}}{s}\right)\frac{(V_{dc}^{ref})^2 - V_{dc}^2}{2} \quad \text{(Eq. 13)}$$

2.2.5. AC voltage control loop

The function of AC voltage control mode is to keep the point of common coupling (PCC) voltage constant and control the active power to/from the PCC. The control law is given by:

$$\Delta V = \frac{K_u}{s}(U_{ref} - U) \quad \text{(Eq. 14)}$$

Where ΔV gives the change in amplitude of the reference voltage VSC.

2.3. Frequency control loop

The frequency control loop has been proposed by several authors [25, 26] and [27] in the literature and all the proposed strategies are based on the same principle, namely: each frequency variation generates a proportional power variation response of the converter. The difference between the works of these authors lies on the overall control of the VSC-MTDC system because the basic principle is based on the application of a single VSC converter. The control strategy adopted in this work is the same as that of the above-mentioned authors.

Its operating principle is very similar to that of voltage drop. A converter equipped with a frequency drop regulator participates in the frequency regulation of the alternating network to which it is connected and modifies its power reference by following the characteristic line whose slope is $1/k_f$ where k_f corresponds to the frequency drop parameter:

$$\Delta P_{f_i}^* = \frac{1}{k_{f_i}}\Delta f_i \quad \text{(Eq. 15)}$$

Where:

- $\Delta P_{f_i}^*$ is the power reference deviation generated by the frequency drop regulator of the i^{th} VSC-HVDC system converter. If $\Delta P_{f_i}^*$ positive then we have an injection of power from the DC network to the AC network, negative otherwise.

- k_{f_i} is the frequency drop parameter of the i^{th} Converter, $k_{f_i} > 0$.

- Δf_i is the variation in frequency of the alternating network connected to the i^{th} converter relative to its frequency reference $\Delta f_i = f_i^* - f_i$.

Based on the PSCS power synchronization loop (Block diagram):

$$\omega t = \Delta\theta + \omega_{ref} \dots\dots\dots\dots t \quad \text{(Eq. 16)}$$

$\omega t - \omega_{ref} t = \Delta\theta$ Still, according to the power synchronization loop we have:

$$\frac{d\Delta\theta}{dt} = K_p(P_{ref} - P)\dots\dots\dots\dots \quad \text{(Eq. 17)}$$

$$d\Delta\theta = K_p(P_{ref} - P)dt$$

$\Delta\theta = K_p(P_{ref} - P)t$ By replacing the expression in Eq 2.30, we have:

$$\omega t - \omega_{ref} t = k_p(P_{ref} - P)$$

$$\Delta\omega = k_p(P_{ref} - P)$$

$$\Delta\omega = k_p(\Delta P_\omega^*)$$

$$\Delta f = k_f \Delta P_f^{\dots\dots\dots\dots *} \quad \text{(Eq. 18)}$$

Therefore, for the i^{th} converter we have the frequency variation of the AC network to which it is connected by:

$$\Delta f_i = K_{f_i} \Delta p_{f\dots\dots\dots\dots i}^* \quad \text{(Eq. 19)}$$

k_{f_i} is the frequency drop parameter of the i^{th} Converter,

Thus, there is a droop relationship between the frequency and the output power of the i^{th} converter, which is the same as that of the primary frequency regulation of a synchronous generator. So, the frequency of VSC station is adjustable, which can synchronize with other AC networks.

3. Results and discussions

3.1. Description of MTDC system of 5 CA countries and Nigeria

This section illustrates the behavior of a 6-terminal MTDC system interconnecting six AC networks. The AC networks of the system are the weak (2 < SCR < 3) and very weak (SCR less than 2) AC networks. The converters are controlled using the dual control technique. Figure **5** shows the block diagram of the MTDC system in Simulink.

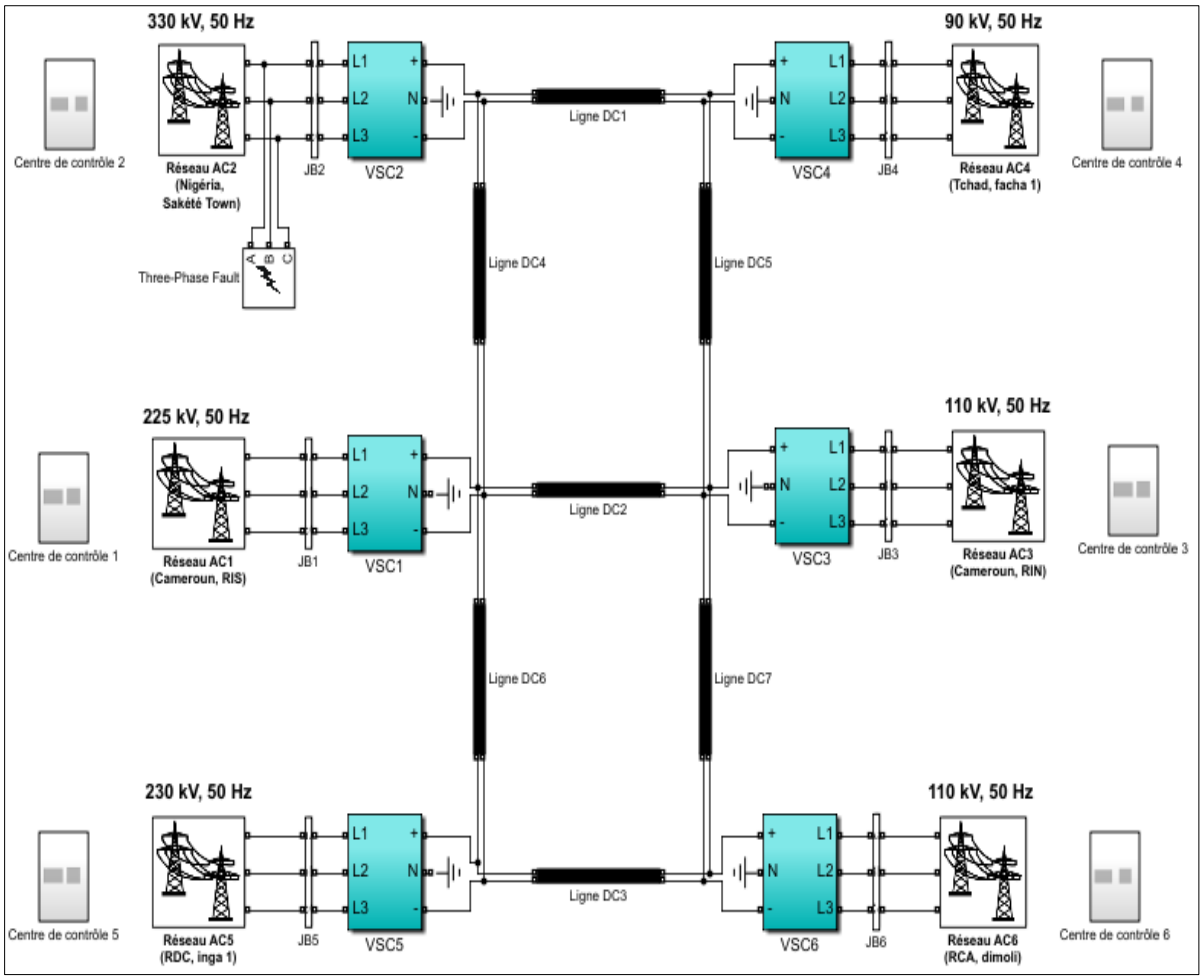

Figure 5 Block diagram of the MTDC system in Simulink

The block diagram of the MTDC system in Simulink presents an interconnection of 6 converters of VSC technology (±100 kV DC) is used to transmit power between 6 AC networks corresponding to the electricity networks of some countries in Central Africa, namely Cameroon (SIN and NIN), Nigeria, Chad, Central African Republic, and Democratic Republic of Congo all with nominal characteristics.

In addition to the converters, the VSC station includes the AC side: the step-down and step-up transformers, the AC filters, and the DC side: the capacitors, the DC filters.

The rectifiers and inverters are interconnected by cables of different distances (i.e. 2 pi sections). A circuit breaker is used to apply a three-phase ground fault on the AC side of the inverter.

Tables 2 and 3 respectively show the initial nominal and reference values of each VSC-MTDC converter station and the lengths (approximate values) of the DC lines.

Table 2 Initial and reference values of each station

Converter	**VSC1**	**VSC2**	**VSC3**	**VSC4**	**VSC6**	**VSC5**
P_n (MW)	388	200	72	60	75	351
P_{ref} (MW)	388	200	72	60	75	351
Q_{ref} (MVAR)	0	0	0	0	0	0

Table 3 Length of DC lines

Line	DC1	DC2	DC6	DC4	DC5	DC7
Length (km)	515	700	650	500	720	450

3.2. AC1 network side performance under normal conditions

Figure **6** illustrates the performance on the AC1 or SIN Cameroon network side under normal conditions.

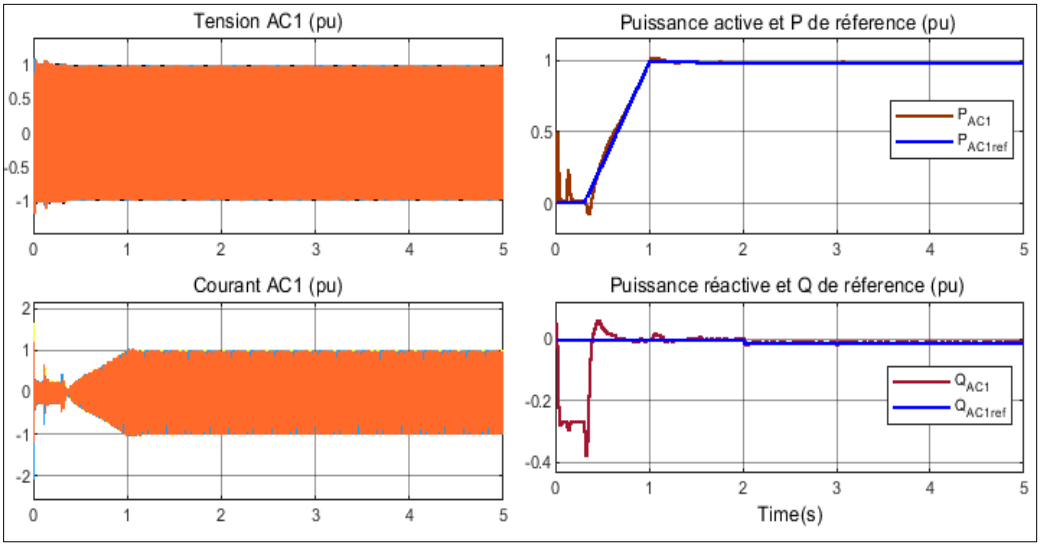

Figure 6 Performance on the AC1 network side under normal conditions

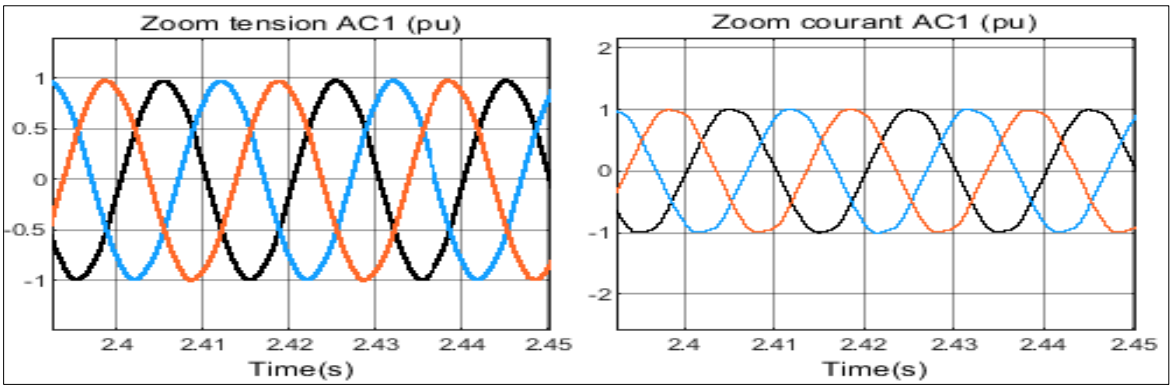

Figure 7 Zoom on the voltage and current of the AC1 network

We can observe on the AC1 network or the Southern Interconnected Network of Cameroon that the voltage and current practically stabilize at a time t = 1 s. Just as the measured active and reactive power also stabilize at this time. We can also observe the active power of the AC1 network which is positive, meaning that the SIN network of Cameroon through the VSC1 station injects power into the MTDC network with a value of 1 pu, i.e. its total available injectable power 388 MW in steady state and also a reactive power with a very interesting value of around -0.01 pu.

3.3. Performance on the AC2 network side under normal conditions

Figure **8** illustrates the performances on the AC2 side or on the Nigerian network side at the Sakété Town substation under normal operating conditions.

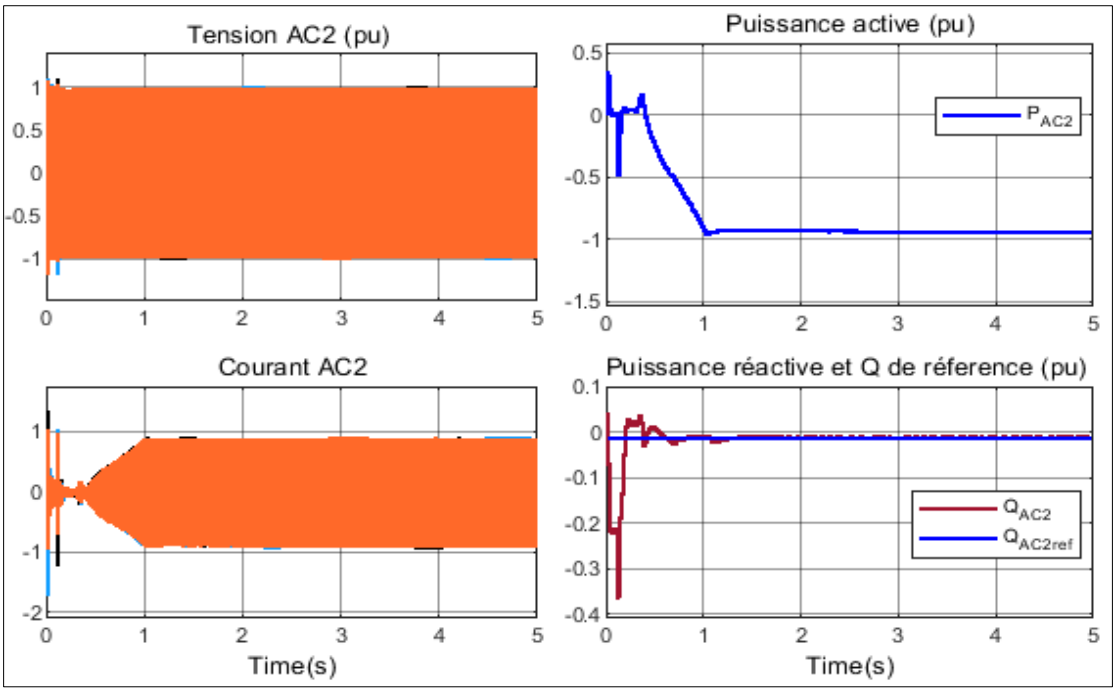

Figure 8 Performance on the AC2 network side under normal conditions

We can also observe from the AC2 network or the Nigerian network that the voltage and current stabilize at t = 1s. We observe that the active power received from the MTDC system which is negative with a value of -0.9 pu approximately, i.e. a compensating active power of 180 MW and a reactive power follows the reference power, i.e. 0 MVAR in steady state.

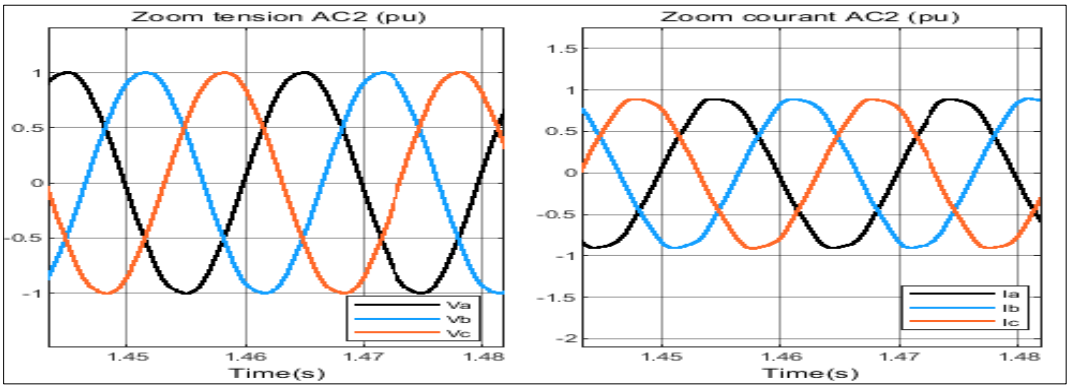

Figure 9 Zoom on the voltage and current of the AC2 network

3.4. Performance on the AC6 network side under normal conditions

Figure **10** illustrates the performance of the Central African network under normal operating conditions.

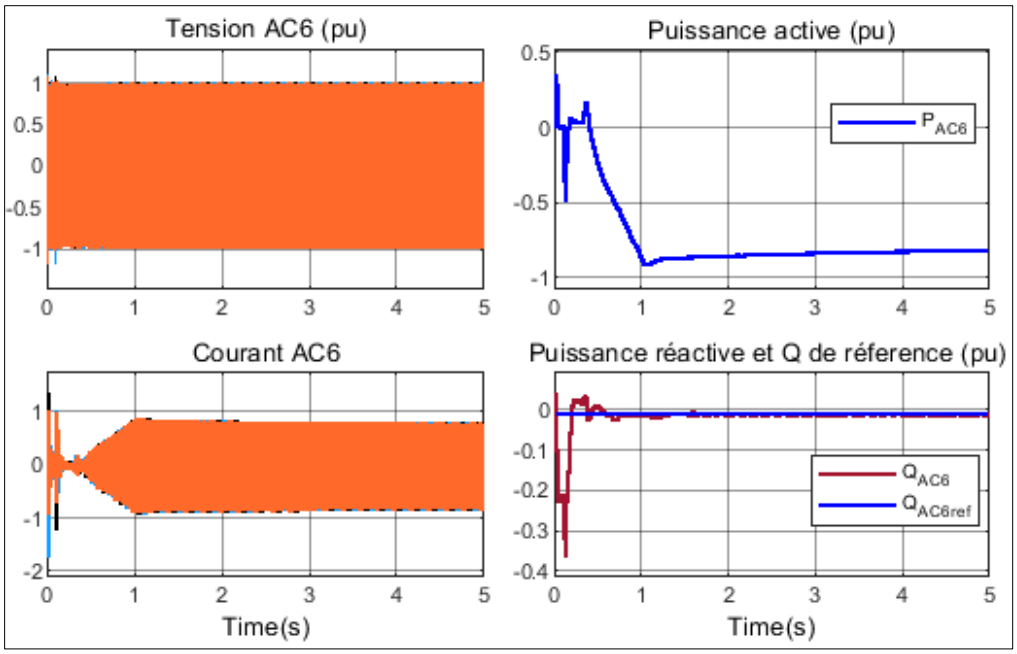

Figure 10 AC6 network side performance under normal conditions

We observe from the CAR network that the system stabilizes at a time of approximately 1.1s and the active power received from the MTDC system more precisely from the Congolese network which is negative with a value of -0.6 pu or a compensating active power of 45 MW and a reactive power which follows the reference power, i.e. 0 MVAR in steady state.

3.5. Performance of VSC1 and VSC2 controllers in normal operation

Figure **11** illustrates the performance of the VSC1 station controller under normal operating conditions.

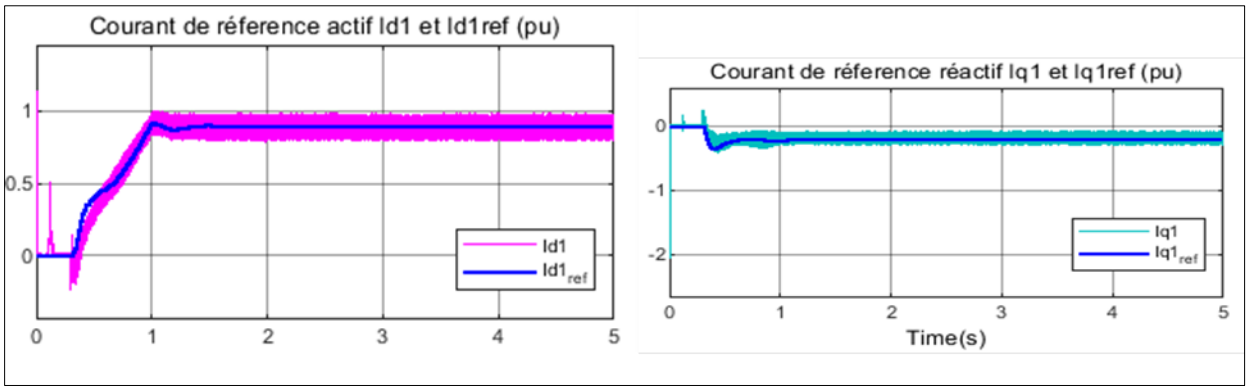

Figure 11 Performance of the VSC1 controller

Figure **12** illustrates the performance of the VSC2 station controller under normal operating conditions.

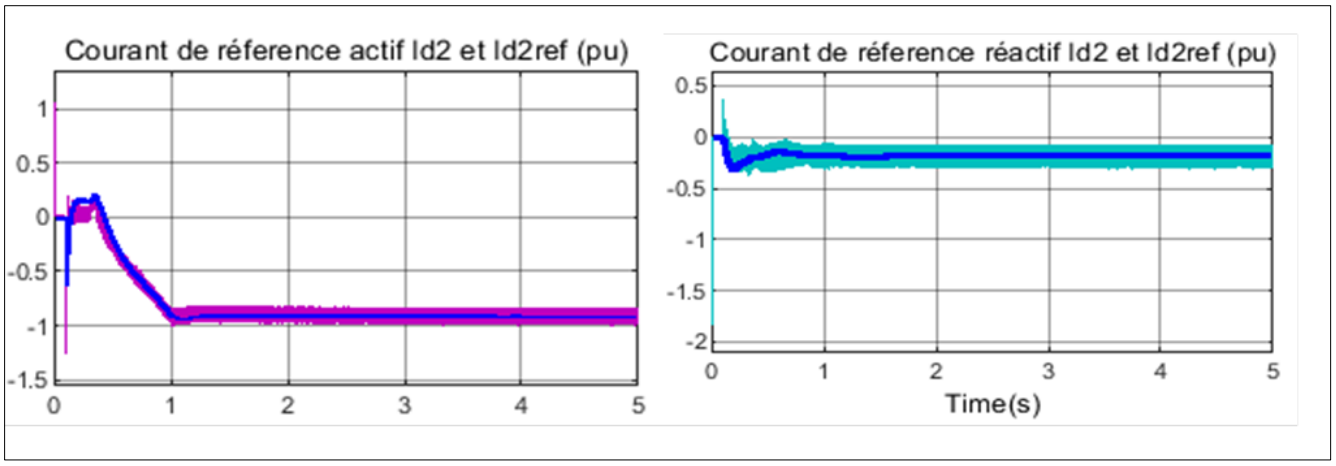

Figure 12 Performance of the VSC2 controller

From Figures 11 and 12, we can observe that the active current references of the different controllers have the form of the active power of the VSC stations and the reactive current references, that of the reactive power. Seen from the AC side in normal operating mode, we can therefore say from Figures 8, 9, 10, 11 and 12 that the MTDC system is stable and respects the standard with regard to the admissible margin of the voltage which is of ±1% excluding tax. In this case, the voltage of the different AC networks is at 1pu, i.e. 225 kV, 330kV, and 110kV respectively for SIN, Nigeria, and RCA.

On the DC side, the DC voltage and the DC power circulating in the DC bus are indicated in the figures below.

3.6. DC rated performance of VSC1 under normal conditions

Figure **13** illustrates the pole-to-ground and pole-to-pole DC voltages at the VSC1 output under normal operating conditions.

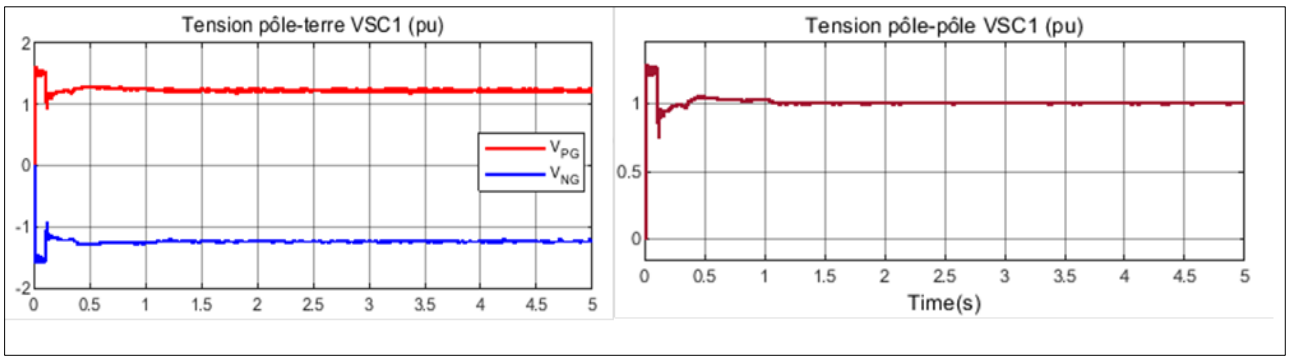

Figure 13 Direct pole-to-earth and pole-to-pole voltages on the VSC1 side

At the VSC1 output, the pole-pole DC voltage is 1pu or 200kV and the pole-earth voltage is 1.1pu or a voltage slightly higher than ± 100kV.

Figure **14** illustrates the power at the output of VSC1 under normal operating conditions.

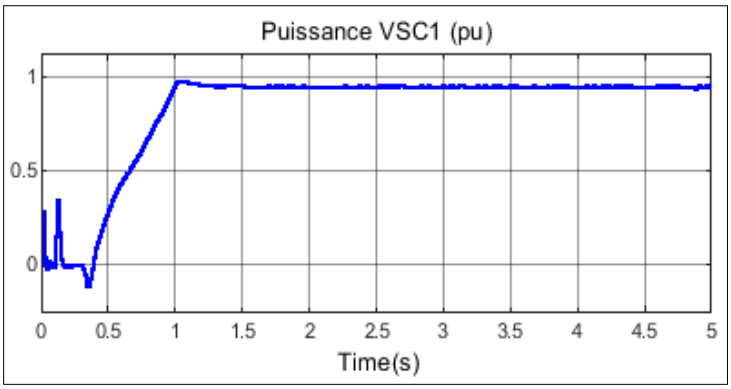

Figure 14 Continuous power output from VSC1

We see in **Figure 14** an injection of DC power into the MTDC network, which is 0.9pu, i.e. a continuous power of 180MW.

DC rated performance of VSC2 under normal conditions

Figure 15 illustrates the pole-to-ground and pole-to-pole DC voltages at the VSC2 output.

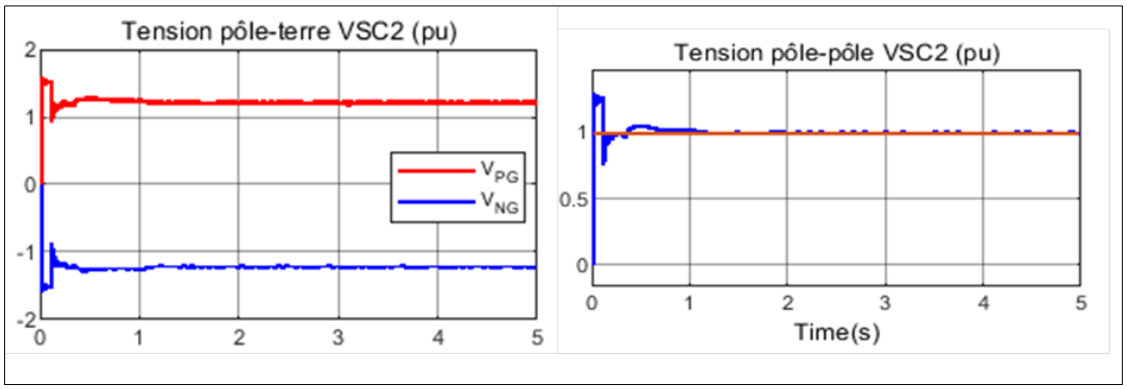

Figure 15 Direct pole-to-earth and pole-to-pole voltages on the VSC2 side

Figure **16** illustrates the power at the VSC2 input under normal operating conditions.

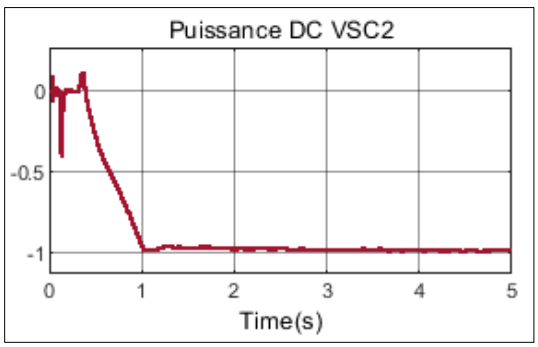

Figure 16 Continuous power input to VSC2

We can see from Figure **16** the reception of a continuous power from the MTDC network which is approximately 0.9pu or a continuous power of 180MW in the direction for the VSC2 station connected to the Nigerian network.

3.7. DC rated performance of VSC6 under normal conditions

Figure **17** illustrates the pole-to-ground and pole-to-pole DC voltages at the VSC6 output under normal operating conditions.

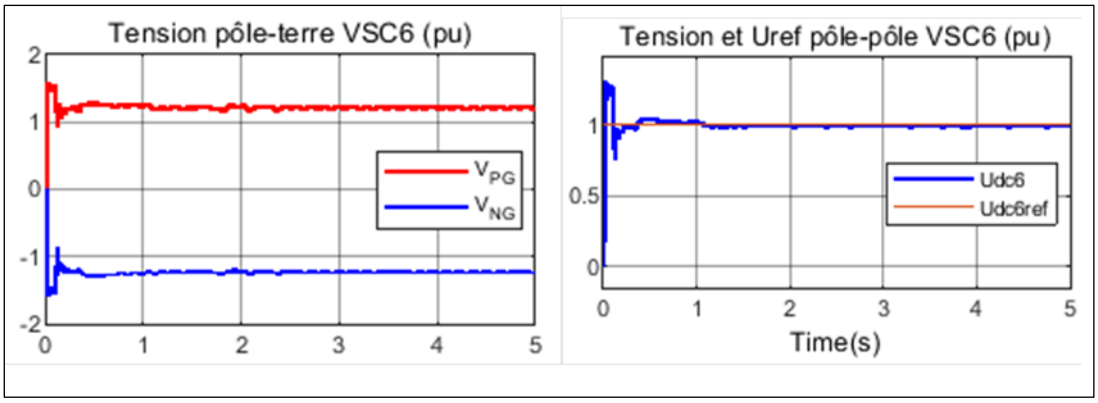

Figure 17 Direct pole-to-earth and pole-to-pole voltages rated VSC6

At the output of VSC1 according to **Figure 17:** the pole-pole direct voltage is 1pu or 200kV and follows the set voltage at t = 1s which is the time when the stability of the system begins and the pole-voltage earth is 1.1pu, i.e. a voltage slightly higher than ± 100kV. Figure **18** illustrates the power at the input of the VSC6 connected to the Central African network under normal operating conditions.

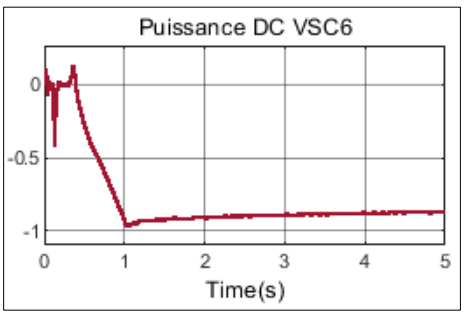

Figure 18 Continuous power input to the VSC6

From **Figure 18,** we observe a continuous power reception from the MTDC network which is approximately 0.6pu, i.e. a continuous power of 45MW in the direction of the VSC6 station connected to the Central African network from the DRC.

For this scenario the references [10] , [28] in their work have practically the same result as ours, that is to say in steady state the system is stable.

- **Scenario 2:** Case of power withdrawal from an AC network

With a view to assessing the flexibility and capacity of the system to cope with disturbances, a simulation is carried out in a case where an unexpected load withdrawal occurs in the AC2 network and the response of the system to the resulting from this simulation are presented in **Figure 19 and 20.**

3.8. Performance of the SIN network side system in Cameroon

Figure **19** illustrates the performances on the AC1 side during scenario 2.

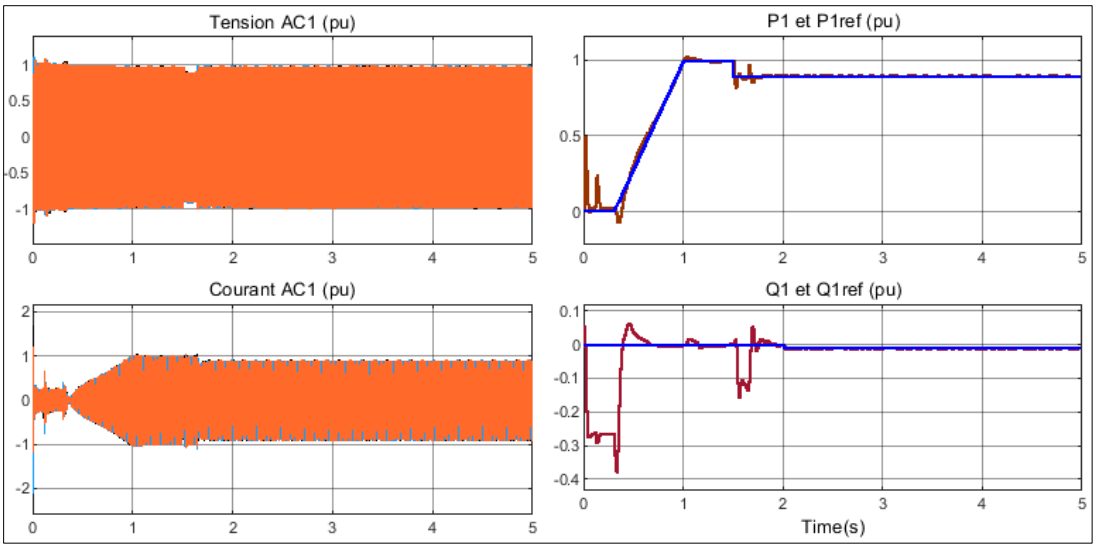

Figure 19 Performance on the AC1 side during scenario 2

From **Figure 19,** we see that at t = 1.5s, a decrease in the current AC1 and the power transmitted in the MTDC system is observed by a value of -0.1pu hence the decrease of 1pu to 0.9pu. The system stabilizes in approximately 0.3 seconds after this incident. Likewise, the reference reactive power also drops from 0 to -0.01pu at t = 2s and on the reference DC voltage on the side of the VSC2 station decreases from 1pu to 0.95pu.

3.9. System performance on the Nigerian network side

Figure **20** illustrates the performances on the AC2 side during scenario 2.

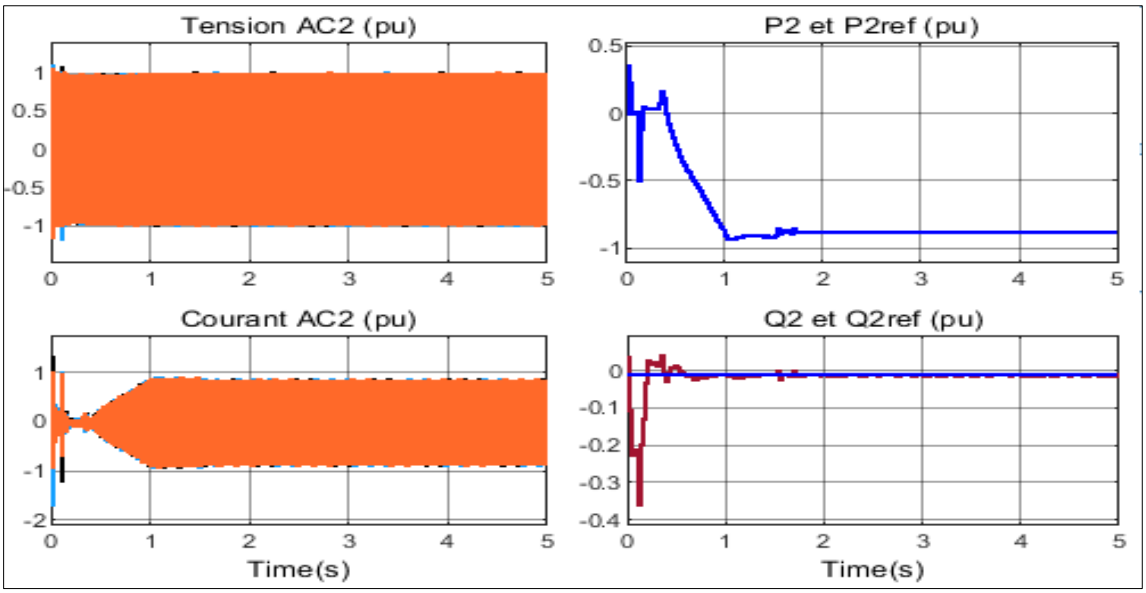

Figure 20 Performance on the AC2 side during scenario 2

We also note (figure **20)** a reduction in the power received from the MTDC of a value of approximately 0.1pu or 18MW at t = 1.5s.

The results obtained from scenario 2 are also similar to the results obtained by [23] with the same system response except that in its case instead of a load removal it is rather an addition of power in the network.

- **Scenario 3:** Case of fault on an AC network

In this simulation to check the reliability of the system, a three-phase fault occurs on the AC2 network at t = 1s, thus causing an imbalance in this AC network for a duration of 0.5s, the fault elimination time.

3.10. AC2 network performance during and after the fault

Figure **21** illustrates the AC2 network voltage and current during and after the fault.

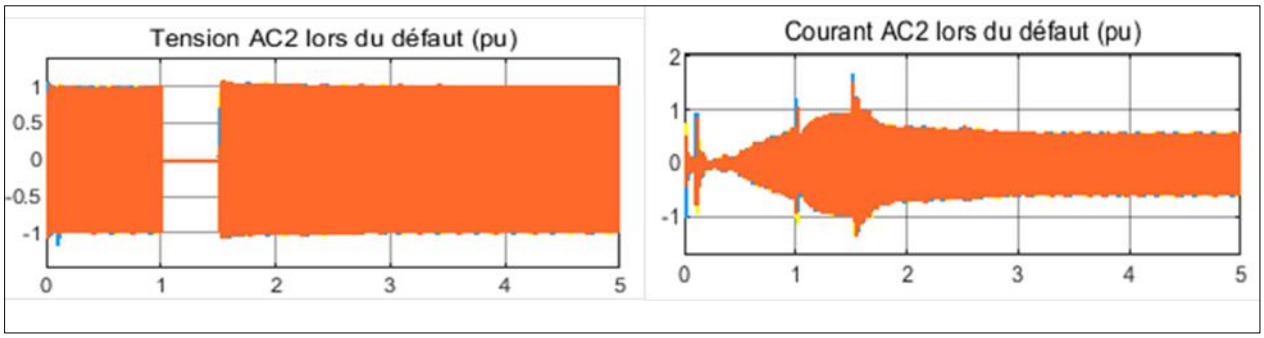

Figure 21 AC2 network voltage and current during and after the fault

We can see from **Figure 21** that during the fault, the AC voltage of the VSC2 converter is practically zero, the current passing through it is limited to 1pu thanks to the current limiting loop of the PSCS, and a current peak of one duration of about 0.01s is observed after the fault is cleared and the steady state of the system is reached again.

3.11 AC1 network performance during and after the fault

Figure **22** illustrates the AC1 network voltage and current during and after the fault

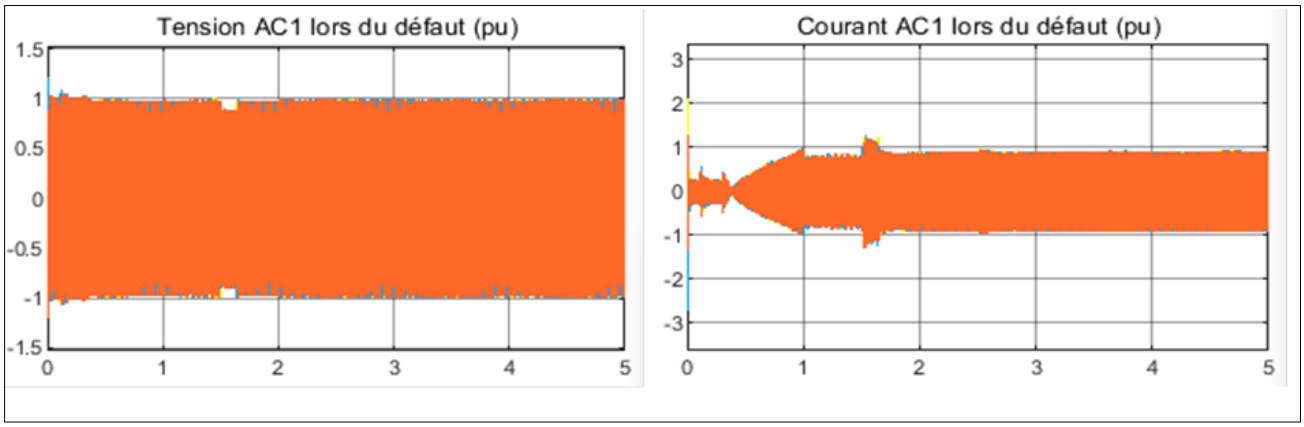

Figure 22 AC1 network voltage and current during and after the fault

On the AC1 side, we just open a small variation of around 0.1s during the fault and after eliminating the fault the system resumes its normal operating mode.

3.11. DC side performance of VSC2 station during and after the fault

Figure **23** illustrates the pole-to-ground and pole-to-pole DC voltage at the input of the VSC2 station during and after the fault.

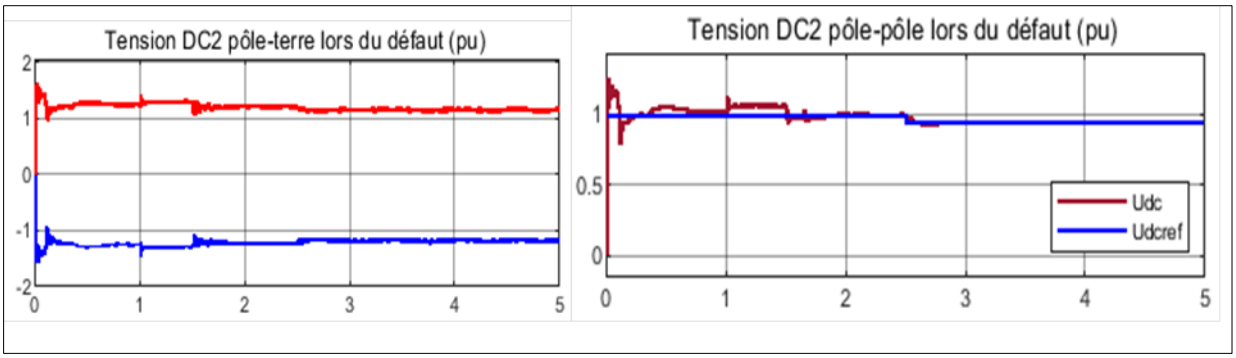

Figure 23 Pole-to-earth and pole-to-pole DC voltage during and after the fault

We observe from **Figure 23** that the pole-to-pole DC voltage increases by about 1.1pu above the reference voltage because the DC side capacitance is excessively charged and also due to output power losses. One of the loops of the PSCS, more precisely the direct control loop of the direct voltage (in the VSC1 station) attempts to limit the DC voltage to the reference DC voltage.

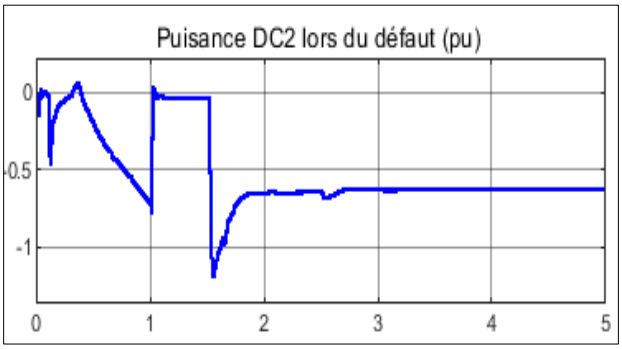

Figure 24 DC power transmitted to the VSC2 station during and after the fault

We can observe from **figure 24** the continuous power transmitted to the VSC2 station is practically zero and reception continues directly after the fault is cleared.

3.11.1. DC side performance of the VSC3 station during and after the fault

Figure **25** illustrates the pole-to-ground and pole-to-pole DC voltage at the VSC3 station output during and after the fault.

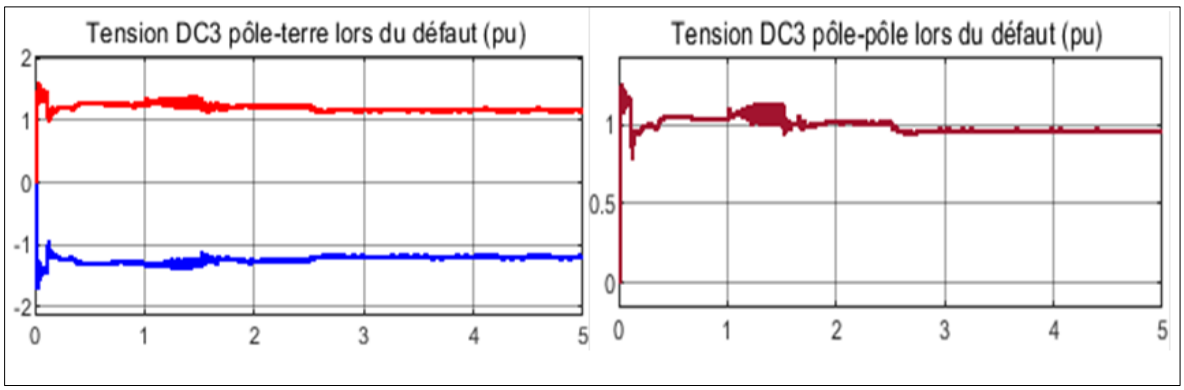

Figure 25 Pole-to-earth and pole-to-pole DC voltage during and after the fault

We observe from **Figure 25** a slight increase in the pole-to-pole DC voltage, and also an increase of about 0.1pu in the pole-to-ground DC voltage above the reference voltage range because the DC side capacitance is overloaded as in the

previous case. The direct voltage control loop installed in the VSC3 station attempts to limit this voltage to its reference voltage. Figure **26** illustrates the DC Power output from the VSC3 station during and after the fault

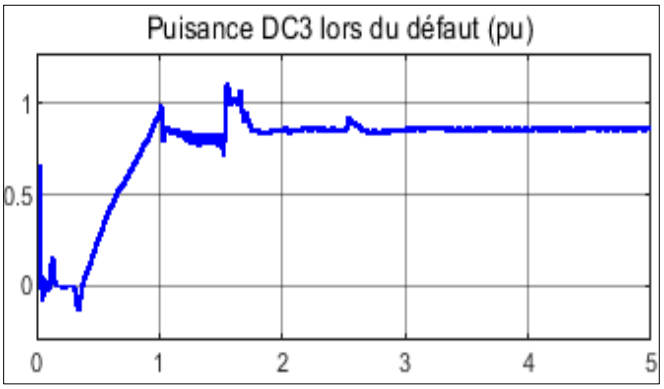

Figure 26 DC power output from the VSC3 station during and after the fault

From **Figure 26,** we observe a power injection of approximately 0.3pu into the AC3 network coming from the surplus stored by the AC1 network during the fault and once the fault is eliminated, it returns to its normal operating position by transmitting its capacity in to other network of the MTDC system.

List of abbreviations

- **AC :** Alternating Current
- **AVC:** Alternating Current Controller
- **PSL :** Power Synchronization Loop
- **HVAC :** High Voltage Alternating Current
- **D.C. :** Direct Current
- **GTO :** Gate Turn-Off Thyristor
- **HV :** High Voltage
- **HVAC:** High Voltage Alternating Current
- **HVDC:** High Voltage Direct Current
- **IGBT:** Insulated Gate Bipolar Transistor
- **LCC :** Line Commutated Converter
- **MMC:** Modular Multi-level Converter
- **MTDC:** Multi-terminal Direct Current
- **PCC :** Point of Common Coupling
- **PLL :** Phase Lock Loop
- **pu:** Per unit
- **PWM:** Pulse Width Modulation
- **EIN:** Eastern Interconnected Network
- **NIN:** Northern Interconnected Network
- **SIN:** Southern Interconnected Network
- **EETN:** Electric Energy Transmission Network
- **PACS:** Power Angle Control Strategy
- **VDCS:** Voltage Drop Control Strategy
- **FCS :** Frequency Control Strategy
- **MSCS :** Master Slave Control Strategy
- **TMCS:** Tension Margin Control Strategy
- **SCR :** Short Circuit Ratio
- **PSCS:** Power Synchronization Control Strategy
- **VCS :** Vector Control Strategy
- **TUE :** Technical Union of Electricity
- **VSC :** Voltage Source Converter

4. Conclusion

The feasibility study of an interconnection of electrical energy transmission networks: Case study of 04 countries of Central Africa and Nigeria had the main objective of carrying out an interconnection and solving the problem of stability of electricity networks. transmission of electrical energy to the countries of Central Africa and Nigeria using the new HVDC electrical energy transmission technology. The results of the simulations obtained confirm the effectiveness of the MTDC system in interconnecting EETN with different parameters. With the model studied, fluctuations or instabilities due to variations in frequency or voltage and faults coming from an AC network of the system like the AC2 network (Nigerian network) that we have simulated are corrected from the MTDC system implemented. place. The implementation of our MTDC system in the sub-region will not only make it possible to avoid energy losses, stability and reliability problems of our EETN but also to reduce as much as possible numerous load shedding, the costs of electricity and promote energy integration. In order to complete this study, it would be interesting to examine the communication aspect of the different terminals for good coordination and efficiency of the proposed MTDC system and also extend the terminals this time with all the countries of Central Africa and Nigeria

Compliance with ethical standards

Disclosure of conflict of interest

No conflict of interest to be disclosed.

References

[1] J. Machowski, Z. Lubosny, JW Bialek, and JR Bumby, Power system dynamics: stability and control . John Wiley & Sons, 2020.

[2] NM Kangwa, C. Venugopal, and IE Davidson, "A review of the performance of VSC-HVDC and MTDC systems," in 2017 IEEE PES PowerAfrica , 2017, pp. 267-273: IEEE.

[3] J. Dai, S. Akkari, and M. Petit, “Voltage control in an HVDC network,” revue 3EI, no. 73, 2013.

[4] TM Haileselassie, T. Undeland, and K. Uhlen, “Multiterminal HVDC for offshore windfarms–control strategy,” 2009.

[5] C. Dierckxsens, K. Srivastava, M. Reza, S. Cole, J. Beerten, and R. Belmans, "A distributed DC voltage control method for VSC MTDC systems," Electric Power Systems Research, vol. 82, no. 1, pp. 54-58, 2012.

[6] J. Binkai and W. Zhixin, “The key technologies of VSC-MTDC and its application in China,” Renewable and Sustainable Energy Reviews, vol. 62, p. 297-304, 2016.

[7] L. Zhang, “Modeling and control of VSC-HVDC links connected to weak AC systems,” KTH, 2010.

[8] S. Li, TA Haskew, and L. Xu, “Control of HVDC light system using conventional and direct current vector control approaches,” IEEE Transactions on Power Electronics, vol. 25, no. 12, pp. 3106-3118, 2010.

[9] L. Zhang, L. Harnefors, and H.-P. Nee, “Power-synchronization control of grid-connected voltage-source converters,” IEEE Transactions on Power systems, vol. 25, no. 2, pp. 809-820, 2009.

[10] K. Seena and T. Sindhu, “Power synchronization control of VSC-HVDC transmission for weak AC Systems,” International Journal of Power System Operation and Energy Management, vol. 2, pp. 2231-4407, 2011.

[11] Ofgem, “Electricity interconnectors ofgem.”

[12] S. Loubna, “Study of a 90 KV high voltage energy transmission network,” 2017.

[13] M. Cepeda, M. Saguan, D. Finon, and V. Pignon, “Generation adequacy and transmission interconnection in regional electricity markets,” Energy Policy, vol. 37, no. 12, pp. 5612-5622, 2009.

[14] D. Juma, J. Munda, and C. Kabiri, “Progress in grid interconnection in East Africa: Challenges, Experiences and Opportunities,” in 2020 IEEE PES/IAS PowerAfrica , 2020, pp. 1-5: IEEE.

[15] A. Berboucha and K. Ghedamsi, “Power Transmission Between Two Asynchronous Grids Using HVDC Technology,” in The 4th International Seminar on New and Renewable Energies , 2016, pp. 1-6.

[16] F. Deustachio, “The challenges of HVDC systems in electricity transmission networks,” Dissertation presented with a view to obtaining EU, Information and communication for engineers, National Conservatory of Arts and Crafts, Grenoble, France , 2013.

[17] J. Setreus and L. Bertling, "Introduction to HVDC technology for reliable electrical power systems," in Proceedings of the 10th International Conference on Probablistic Methods Applied to Power Systems , 2008, pp. 1-8: IEEE.

[18] S. Messalti, “Analysis of the transient stability of high voltage direct current transmission networks (HVDC-FACTS),” 2018.

[19] EWE Association, Pure power-wind energy targets for 2020 and 2030 . Ewea, 2011.

[20] E. Joncquel, “Information on direct current energy transport,” Technique de l’enseignement D 4 763 .

[21] Ali Berboucha, “Power transmission between two asynchronous networks using HVDC technology” October 25, 2016

[22]] C.D. Jedili, "study of a high voltage direct current (HVDC) energy transmission system," Mohamed Boudiaf-M'Sila University, 2007.

[23] H. Chen, C. Wang, F. Zhang, and W. Pan, "Control strategy research of VSC based multiterminal HVDC system," in 2006 IEEE PES Power Systems Conference and Exposition , 2006, pp. 1986-1990: IEEE.

[24] S. Cole, J. Beerten, and R. Belmans, “Generalized dynamic VSC MTDC model for power system stability studies,” IEEE Transactions on power systems, vol. 25, no. 3, pp. 1655-1662, 2010.

[25] TM Haileselassie and K. Uhlen, "Primary frequency control of remote grids connected by multi-terminal HVDC," in IEEE PES General Meeting , 2010, pp. 1-6: IEEE.

[26] J. Machowski, J. Bialek, J. R. Bumby, and J. Bumby, Power system dynamics and stability . John Wiley & Sons, 1997.

[27] N. R. Chaudhuri, R. Majumder, and B. Chaudhuri, “System frequency support through multi-terminal DC (MTDC) grids,” IEEE Transactions on Power Systems, vol. 28, no. 1, pp. 347-356, 2012.

[28] S. Houndedako, K. Kpode, A. Vianou, and C. Espanet, "Study for synchronization of the electrical networks of the electrical community of Benin (CEB): case of the Volta River Authority (VRA) and transmission Company of Nigeria (TCN),” Afrique Science: International Journal of Science and Technology, vol. 10, no. 2, 2014.